Stresses in peripheral arteries following stent placement: A finite element analysis

Journal:	*Computer Methods in Biomechanics and Biomedical Engineering*
Manuscript ID:	GCMB-2007-0044.R2
Manuscript Type:	Original Article
Date Submitted by the Author:	n/a
Complete List of Authors:	Early, Michael; Trinity College Dublin, Mechanical Engineering Lally, Catriona; Dublin City University, School of Mechanical and Manufacturing Engineering Prendergast, Patrick; Trinity College Dublin, Mechanical Engineering Kelly, Daniel; Trinity College Dublin, Mechanical Engineering
Keywords:	Peripheral Artery, Stent, Finite Element Analysis

Computational Methods in Biomechanics and Biomedical Engineering

Vol. X, No. X, Month 200X, 000–000

Article type: Research Article

Stresses in peripheral arteries following stent placement: A finite element analysis

Michael Early[a], Catriona Lally[b], Patrick J. Prendergast[a] and Daniel J. Kelly[a*] [where * denotes corresponding author, see below]

[a]*Trinity Centre for Bioengineering, Department of Mechanical and Manufacturing Engineering, Trinity College Dublin, Dublin 2, Ireland;*

[b]*School of Mechanical and Manufacturing Engineering, Dublin City University, Glasnevin, Dublin, Ireland*

The success of stents to restore blood flow in atherosclerotic peripheral arteries is low relative to coronary arteries. It has been shown that joint flexion induces a mechanical environment that makes stent placement in these arteries highly incompatible, and damage and destruction of stents has been recorded. However, the effect of this environment on the stresses in the arteries is unknown. It is hypothesised that the stresses induced in arteries as a result of this mechanical environment could be sufficient to explain the relatively low success rates. To investigate this hypothesis, a finite element model of the stent-artery interaction was developed. Following stent expansion, bending was simulated by applying a displacement boundary condition to the artery. It is found that high stresses occur at the proximal/distal ends of the stent. As stress and vascular injury are hypothesised to cause restenosis, the results presented here suggest that the mechanical environment of peripheral arteries could be the predominant cause of high restenosis rates.

Keywords*:* peripheral stent; finite element analysis, artery bending

Title Page Footnote:

---

*Corresponding author. Email: kellyd9@tcd.ie

1. Introduction

The placement of stents in arteries to relieve blockages caused by atherosclerosis has proved highly successful in coronary arteries. Restenosis rates have been reported at below 10% from six month follow ups for bare metal stents (Jorgensen *et al.*, 2003, Moer *et al.*, 2001), while more recent studies have shown that even patients with acute myocardial infarction experience binary restenosis rates of 21.3% for bare metal stents and 9.3% for drug eluting stents after one year (Menichelli *et al.*, 2007). However, similar treatments have proved less successful in peripheral arteries, or arteries outside the heart. It has been shown that the iliac artery experiences more intimal hyperplasia than the coronary artery, but with less subsequent restenosis in porcine tests. The differences in restenosis rates between the two types of artery are not statistically significant (Krueger *et al.*, 2006). Distal to the iliac arteries, the differences in restenosis rates between peripheral and coronary arteries is more evident. The superficial femoral artery, for example, has long-term patency rates that are reported to vary between 8 and 89% (Matsi *et al.*, 1995, Mukherjee *et al.*, 2001). Strecker *et al* report 2 year patency rates of 51%, reducing to 48% after 3 years (Strecker *et al.*, 1997). The use of more flexible self-expanding nitinol (shape memory alloy) stents has improved performances somewhat, but binary restenosis is still reported to be 24% at 6 months (compared with 44% for PTA alone) (Schillinger *et al.*, 2006). Stent fracture has also been reported in case studies (Babalik *et al.*, 2003, Solis *et al.*, 2006), while a broader study showed a stent fracture rate of 24.5% in peripheral arteries at a mean follow up of 10 months (Scheinert *et al.*, 2005). While almost half of the fractures were classified as minor (single strut fracture), a quarter were major (complete separation of stent segments) and a strong correlation was shown between stent fracture and restenosis. Primary patency rates at 12 months were 84.3% without stent fracture and 41.1% where stent fracture occurred. This study also showed the importance of stent design and the number of stents implanted in fracture rates, as well as demonstrating that fracture is more likely in longer stented lesions. The latter finding is supported by Strecker *et al* (Strecker *et al.*, 1997), who showed that restenosis rates are higher

where longer stents are used. There is little data available for popliteal and tibial angioplasty and stenting procedures, though it has been reported that high initial success rates are followed by poor long-term results (Mukherjee *et al* 2001). It is reported that femoropopliteal arteries, as well as being more susceptible to restenosis, account for 50% of peripheral obstructive lesions (Solis *et al.*, 2006).

The reasons for the relatively high failure rates of stents placed in the femoral and popliteal arteries are not fully understood. However there are a number of known differences between coronary and peripheral arteries which may help to explain the variation in success rates; the first is size. Stents implanted into coronary arteries are typically less than 4mm in diameter, while stents implanted into peripheral arteries can be up to 10mm in diameter, depending on location. Blockages in peripheral arteries often require the use of longer stents compared with coronary arteries, with single peripheral stents commonly being as long as 80mm. A second potentially important difference is the variation in vessel wall thickness and composition with distance from the heart. Generally, arteries close to the heart are more elastic to allow for volumetric change during pulsatile blood flow, while peripheral arteries are more muscular and do not distend as much. Although coronary arteries, classified as muscular arteries, are an exception to this rule, their composition is still different to peripheral arteries (Martini, 2004). A third key difference between coronary and peripheral arteries in the lower limb is the mechanical environment; both are subject to pulsatile loading cycles but the magnitude and shape of the waveforms can differ. The maximum and minimum pressures are comparable in the coronary and iliac arteries (Mills *et al.*, 1970) whereas other components of loading are quite different. Coronary arteries such as the right coronary artery (RCA) and left anterior descending (LAD) arteries are attached to the myocardium, and as such experience displacements and deformations as the heart beats. The behaviour of an RCA and LAD over two cardiac cycles has been recorded by Ding *et al* (Ding *et al.*, 2000, Ding *et al.*, 2002). Significant displacement, bending and torsion have been reported in both arteries, with

diseased portions of the arteries exhibiting significantly higher average torsion than normal portions of the same vessel. In general, these arterial motions have been investigated in relation to their influence on vessel deformations and hemodynamics (e.g. Ding *et al.*, 2000, Weydahl *et al.*, 2001, Zeng *et al.*, 2003), in particular wall shear stresses, while less is known about the influence of such motions on arterial stresses post-stenting.

The mechanical environment of the peripheral arteries, especially the femoral, popliteal and tibial arteries is influenced by joint movement. Flexion of the knee, for example, can cause occlusion of the popliteal artery due to compression even in healthy patients (Hoffmann *et al.*, 1997). This is because flexion of the knee causes a bending effect in the artery. Bending of arteries typically occurs about a hinge point, which has been defined as the "first curve in the peripheral artery in an acute angle towards the femur that appeared during knee flexion" (Diaz *et al.*, 2004). The concept of a hinge point was first introduced by Duda et al (Duda *et al.*, 2002), who suggested that vessel movement and compression might introduce and develop hinge points in stented arteries. This is expanded upon by Diaz et al (Diaz *et al.*, 2004), who specified the location of hinge points in popliteal arteries affected by PAD and related their formation to knee flexion of up to 100°. While the dynamics of the femoral and popliteal artery segments have not been documented in the same manner as coronary arteries, inspection of angiograms during knee flexion (Diaz *et al.*, 2004, Duerig *et al.*, 2002) suggests greater bending compared with the coronary arteries. The extreme mechanical environment experienced by stents in the popliteal and distal femoral arteries due to joint flexion is documented by Kroger *et al*. (Kroger *et al.*, 2004) and Solis *et al* (Solis *et al.*, 2006). These reviews illustrate how stents are bent by knee flexion, in some cases leading to mechanical failure of the stent. Rosenfield *et al* (Rosenfield *et al.*, 1997) also identify stent compression as the mechanism for restenosis in the superficial femoral artery, although the cause of compression is not identified.

It has been hypothesised that rates of restenosis are related to damage, or injury, in the artery following stent deployment (Schwartz, 1994). Therefore, it can be said that stents which reduce the stress in the arterial wall are less likely to induce restenosis, while factors that increase stress in the artery are likely to promote restenosis. These factors include stent design (Bedoya *et al.*, 2006, Lally *et al.*, 2005, Prendergast *et al.*, 2003), material properties, over expansion of stent (Ballyk, 2006) and possibly bending of the vessel. The finite element method has proved extremely useful in modelling the mechanics of stent expansion and stent-plaque-artery interactions and it has been demonstrated that finite element modelling is useful for analysing stent/wall stress distributions (Takashima *et al.*, 2007). Stent expansion has been modelled using a number of different approaches, including the expansion of the artery beyond the diameter of the stent and subsequent removal of pressure (Lally *et al.*, 2005), application of pressure directly to the internal faces of the stent (Chua *et al.*, 2002, Holzapfel *et al.*, 2005, Migliavacca *et al.*, 2005), and explicit but simplified cylindrical balloon models that use various material models to simulate the changing stiffness of the balloon as it unfolds (Chua *et al.*, 2003, Chua *et al.*, 2004, Gay *et al.*, 2006, Wang *et al.*, 2006). Only recently has the interaction between a folded balloon and stent been modelled (De Beule, 2006, Laroche *et al.*, 2006).

To date, the majority of studies investigating stent-artery interactions have focused on coronary vessels. While the principle of expanding a stent in a peripheral artery is similar, the mechanical environment within peripheral arteries is different to that within coronary arteries due to greater vessel bending caused by joint flexion. It is hypothesised that repetitive joint motion following stenting in peripheral arteries induces excessively high stresses in arterial walls, thereby increasing vessel damage and subsequently promoting restenosis. To test this hypothesis, a finite element model of a stent within a peripheral artery was developed. The stent was expanded in the artery, after which a bending boundary condition was applied. The percentage of tissue volumes within specified stress ranges can then be determined before and after arterial bending. If it

is shown that bending the artery significantly increases its stress state, then it can be said that this bending could be responsible for higher rates of restenosis in peripheral arteries. In addition, the stresses in the stent due to cyclic loading will be investigated.

2. Materials and methods

2.1 Model Geometry

The geometry of the stent modelled is based on a Palmaz design. In its unexpanded state, the stent is 20mm in length and has an outer diameter of 3mm, with a wall thickness of 0.1 mm. The artery is modelled as having a length of 40mm, a diameter of 10 mm (Radegran *et al.*, 2000) and a thickness of 1 mm (Learoyd *et al.*, 1966). The plaque within the artery was modelled as a uniform hollow cylinder, with a thickness following pre-dilation by balloon angioplasty of 0.5 mm and a length of 14.4 mm. The plaque is 5.6 mm shorter than the unexpanded stent, see Fig. 1. A further reduction in computational time was achieved by taking advantage of symmetry and using a one quarter model of the system with symmetrical boundary conditions applied.

2.2 Material models

The material for the stent was simplified as a bi-linear elasto-plastic model based on micro specimens of 316L stainless steel (Wiersma *et al.*, 2006), with a Young's modulus of 188 GPa, and a tangent modulus of 0.513 GPa. The materials for the artery and the stenotic plaque were hyperelastic models described by a Mooney-Rivlin model, given generally as

$$W(I_1, I_2, I_3) = \sum_{i,j,k=0}^{\infty} a_{ijk} (I_1 - 3)^m (I_2 - 3)^n (I_3 - 3)^o \quad (1)$$

The specific form of this equation used here is:

$$W = a_{10}(I_1 - 3) + a_{01}(I_2 - 3) + a_{20}(I_1 - 3)^2 + a_{11}(I_1 - 3)(I_2 - 3) + a_{30}(I_1 - 3)^3 , \quad (2)$$

where the strain invariants, I_1, I_2 and I_3 are functions of the principal stretches, λ_1, λ_2 and λ_3 as follows:

$$I_1 = \lambda_1^2 + \lambda_2^2 + \lambda_3^2$$
$$I_2 = \lambda_1^2\lambda_2^2 + \lambda_1^2\lambda_3^2 + \lambda_2^2\lambda_3^2$$
$$I_3 = \lambda_1^2\lambda_2^2\lambda_3^2 \quad . \quad (3)$$

The parameters, a_{ijk}, are taken from Lally *et al* (Lally *et al.*, 2005).

Three dimensional, eight-node, first order isoparametric elements (Marc type 7) were used for the stent. Nine-node, first order isoparametric elements (Marc type 84) with mixed (full and Herrmann) formulation were used for the artery and the plaque, due to the ability to incorporate Mooney-Rivlin material models with this type of element.

Frictionless contact was assumed throughout, except for the plaque and artery, which were bonded together. A mesh density study was carried out to ensure that the mesh used was sufficiently refined by increasing the number of elements in the artery from 24,000 to 100,000 and 192,000 and analysing the stresses. It was found that peak Von Mises stresses varied by less than 2%, while stress distribution graphs showed volume changes of less than 1% within each specified stress range.

2.3 Boundary Conditions

To reduce the computational cost of modelling the interaction of the stent, balloon, plaque and artery, it was decided to simplify the modelling of the expansion process. This was achieved by applying pressure directly

to the inside faces of the stent elements without modelling a balloon. However, due to the closed cell design of the stent, the finite element model predicted expansion of the extremities at a far greater rate than the centre of the model, leading to incomplete expansion of the stent. This 'flaring' or 'dog-boning' affect is characterised in various ways and reported to different degrees in the literature (Chua *et al.*, 2002, Liang *et al.*, 2005, Migliavacca *et al.*, 2005, Wang *et al.*, 2006), though full expansion of the stent occurs. To simulate the constraint of the balloon, which generally prevents the stent from expanding beyond the specified diameter of the balloon, spring elements were incorporated into the model (see Fig. 1b & c).

The springs had a multi-linear stiffness; the stiffness was very low (0.1 N/m) until the stent reached its nominal diameter, at which stage the stiffness increased sharply to 1,000N/m to prevent further expansion of the stent beyond the diameter of the balloon. These springs were attached to nodes along the centre-line of the stent geometry which were constrained in the radial direction and tied longitudinally to nodes on the stent to allow for foreshortening. Using this approach, it is assumed that the stent was expanded using a non-compliant balloon. For the purpose of this investigation, the bending of the artery was modelled as a simple three-point bending, similar to standard tests carried out to examine the flexibility of stents (Ormiston *et al.*, 2000). This was simulated by expanding the stent in the artery, allowing recoil by removing the pressure, and applying a fixed displacement of 10mm to the distal end of the artery, see Fig. 2. Accounting for symmetry, this is similar to three point bending. This test was run using models of the artery with and without the presence of atherosclerotic plaque. To quantify the stresses in the arterial wall following expansion, recoil and bending, the volumes of stress within particular stress ranges were analysed. This was undertaken by assigning a single stress value to each element, which was defined as the average Von Mises stress within the element. The percentage volume within defined stress ranges was calculated from these results.

3. Results

3.1 Expansion

The result of stent expansion using internal pressure and constraint with spring elements was initial flaring of the stent, with the extremities expanding at a greater rate than the centre, followed by full expansion. This initial flaring causes the crowns at the end of the stent to dig in to, or pinch, the artery wall at an angle (Fig. 3).

Flaring, or dog-boning, is defined by Wang *et al* (Wang *et al.*, 2006) as

$$Dogboning = \frac{D_{Distal} - D_{Central}}{D_{Central}} \times 100\% \quad (4)$$

Where D_{distal} is the diameter at the end of the stent and D_{central} is the diameter at the centre of the stent. Using this formula, it was predicted that dog-boning reached a peak value of 52% when 24% of the expansion process is completed.

Following stent expansion, almost the entire artery is defined as being within a stress range of 0-0.2 MPa, with or without the presence of plaque (Fig. 4 & 5). In the model with plaque present, there is a very small (<0.15%) percentage of the artery volume with a Von Mises stress greater than 0.5 MPa. When the plaque is not present, there are again small amounts at 0.5 MPa or greater, but also slightly larger volumes (1.5%) at greater than 0.9 MPa, see Fig. 5.

3.2 Recoil

Recoil of the stent (the decrease in diameter of the expanded stent once the pressure is removed caused by elastic recovery) results in a reduction in stress in the artery wall. In the model with a plaque, 99.7% of the artery is in the first stress range of 0-0.1 MPa, see Fig. 4. In the model with no plaque, 98.6% is within the same range. However, small volumes of highly stressed tissue remain even after recoil, with an insignificant reduction in volume within this range, see Fig. 5.

3.3 Bending

When the artery is bent around the stent, increased tissue stresses are predicted, see Figs. 4 and 5. With a plaque present, the volume of artery at lower stress levels (<0.1MPa) is reduced from 100% after recoil to 30% after bending. The amount of artery within the high stress ranges also increases, with none of the vessel wall above 0.4 MPa before bending and 11.4% within ranges above 0.4 MPa after bending. The trend is similar when no plaque is present in the model, with 98.5% of the artery below 0.2 MPa before bending and 21% at the same level after bending; none of the artery is stressed above 0.4 MPa before bending, 4.9% is following bending (Figs. 4 & 5). The high peak stresses in the artery are located at the distal/proximal end of the stent both before and after bending, see Fig. 6. When the bending boundary condition is removed and the artery is straightened again, the stress states are almost identical to those before the artery is bent, with the peak stress reducing from 320kPa (before bending) to 153kPa when the bending has been removed. As might be expected, the stresses within an unstented artery due to bending are significantly lower than that predicted

in a stented artery, however interestingly they are generally higher than in the unbent stented artery following expansion (see Fig. 6).

3.4 Stress in Stent

Crimping prior to deployment is not simulated in this model, so it is assumed that the initial stress within the stent is zero. Kröger (Kroger *et al.*, 2004) reported that stent deformation and destruction could result from the mechanical conditions experienced by peripheral stents. This model shows considerable permanent deformation after one cycle and high stresses in the stent, see Fig 7. When bending is applied to the stent, the highest variation in stress occurs close to where two struts are connected, with a peak stress of 376.8 MPa. The stress at this point is 163.2 MPa when bending is not applied, giving a cyclic stress range of 213.6 MPa due to vessel bending.

4. Discussion

Although the difficulties following implantation of stents in peripheral arteries have been documented (Matsi *et al.*, 1995, Mukherjee *et al.*, 2001, Strecker *et al.*, 1997), the reasons for this have never been analysed fully from a biomechanical point of view. The finite element analysis presented in this paper is used to predict the change in stress in the peripheral artery following stenting and bending of the vessel. Bending the artery following stenting significantly increases the stress in the artery with and without a plaque present, with a slightly greater average stress when plaque is present.

Flaring, or dog-boning, as defined by Wang *et al* (Wang *et al.*, 2006), reaches a peak value of 52% when 24% of the stent expansion is complete (Fig. 4). While this is higher than that of 43% reported by Wang *et al* (Wang *et al.*, 2006) for stents with an open-cell design, non-uniform balloon expansion can result in extreme cases of dog-boning with even higher values, the degree of which depends on stent design, balloon length and rate of application of pressure. During expansion, the flaring affect causes the proximal/distal crowns of the stent to be the first parts to impinge on the vessel wall. This occurs at an angle rather than parallel as would happen with ideal expansion, inducing high stress. Although almost uniform expansion of the stent ensues once the nominal inflation pressure has been reached, regions of localised high stresses remain (Fig. 6). This is significant as it has been shown that the manner of stent deployment is important in determining injury (Squire, 2000) and acute vascular injury can occur at the ends of stents (Wang *et al.*, 2006). Therefore the stress within the artery during and after expansion, particularly the peak stresses, depend in part on the expansion characteristics of the stent. When the plaque is present in the artery, it acts as a buffer layer, giving a more uniform circumferential and radial stress distribution within the artery during expansion, though the stress values are higher due to greater radial displacement of the artery. As the artery is stretched further radially it is kept further from the stent by the intermediary layer of plaque. This reduces the affect of the stent crowns that induce high stresses at the ends of the stent. There are still areas of high local stress at the same location, however they are of lower magnitude than the unstenosed artery.

In an artery with no plaque present, small volumes of the artery are at high stresses, greater than 0.9 MPa, after the stent is expanded. The areas of high arterial stress during expansion correlate with the ends of the stent impinging upon the artery due to dog-boning. These stresses remain when the pressure is removed and the stent recoils. When the artery is bent, high stresses occur in the artery distal to the stent as well as the

region at which the artery is in contact with the stent. High stresses are also predicted in this distal region in an unstented artery following bending (see Fig. 6c). The peak stresses in the stented artery following bending are still located at the end of the stent in line with the location of the stent crowns (see Fig. 6b). This could be attributed to the stent 'anchoring' part of the vessel and therefore inducing a high stretch in the tissue immediately adjacent to the stent during bending.

The complete and uniform expansion of the stent *in vitro* requires the use of a non-compliant inflation balloon. A study by Liang *et al* (Liang *et al.*, 2005) showed that using a simplified, cylindrical balloon caused the distal ends of the stent to tilt, pinching the artery wall. This is attributed to the plaque being shorter than the stent, and not providing support for the parts of the stent distal to the plaque. While this is suggested as a factor in increasing vascular injury, it can be shown from the result presented here that even if the stent's eventual deployment is uniform, the path taken is still an important factor in determining vessel stresses. Therefore, to reduce arterial stresses, and hence vessel damage, it is important to minimise flaring during expansion.

The slight difference in the stresses in the artery after bending has been applied and after bending has been removed can be attributed to the plastic deformation of the stent following bending. Because the artery and plaque are modelled as being hyperelastic, if no plastic deformation takes place the stress states after bending and re-straightening would be identical. As knee flexion is necessary for locomotion, it can be said that a stented artery will be subject to a cyclic stress with a high stress state following bending caused by knee flexion, and lower stresses during extension. This cycle, could be sufficient to cause restenosis in peripheral arteries following stenting. Any permanent deformation of the stent and incomplete stent apposition (ISA) would be expected to reduce vessel wall support and influence the blood flow through the artery, possibly

causing turbulence. The changing geometry of the vessel, caused by bending of the artery and by the reduced support from the deformed stent could also affect blood flow. The affects of altered fluid dynamics have not been investigated in this paper.

A S/N (stress/cycle) curve for microscopic samples of 316L stainless steel shows that a stress amplitude less than 420 MPa is required to be within the fatigue limit for a plain specimen with no cracks or notches (Wiersma *et al.*, 2006). Although the stress range calculated for this stent using a bi-linear model shows that the stress range is less than that required for fatigue failure to occur, there are factors which suggest fatigue may be a problem. The effect of a mean stress superimposed onto a cyclic stress on the fatigue characteristics of a material can be accounted for using the Goodman curve/formula as follows:

$$\Delta\sigma_{\sigma m} = \Delta\sigma_0\left(1-\frac{\sigma_m}{\sigma_{TS}}\right) \qquad (5)$$

Where $\Delta\sigma_0$ is the cyclic stress range for failure in N_f cycles under zero mean stress, $\Delta\sigma_{\sigma m}$ is the same for a mean stress of σ_m and σ_{TS} is the ultimate tensile strength. Values of 420 MPa for the stress range and 600 MPa for σ_{TS} for a required fatigue life of one million cycles were taken (Wiersma *et al.*, 2006). Stresses of 393.75 MPa following bending and 146.25 MPa at the same point before bending give a stress range of 247.5 MPa with a mean stress of 270 MPa. This represents the highest mean stress seen in the stent. The 213.6 MPa stress range predicted by the model is slightly less than the value of 231 MPa required to remain below the fatigue limit, suggesting that the stent will not fail by fatigue. However, this factor of safety is likely to be too low for a stent deployed in the real artery with its more complex shape, loading conditions and plaque geometry.

When analysing the results presented here, it is important to consider the assumptions and simplifications that are necessary to model the complex interactions. The arterial model, though suitable for this study, neglects certain aspects of the material behaviour of such tissues (Holzapfel *et al.*, 2000, Holzapfel *et al.*, 2005). There is no curvature along the longitudinal axis of the vessel, and symmetry is assumed. The plaque and artery are modelled as homogenous and isotropic materials. In reality, vessel deformations are complex three dimensional phenomena, rather that simple bending in one plane. In our model the artery is not pre-stressed, and blood pressure is not applied. Stress relaxation occurs relatively quickly in arteries. This stress relaxation, fatigue of the artery and other time-dependant properties are not studied in this paper. Despite these simplifications, the model is believed to be adequate for the purposes of this study, and is valid for comparative studies.

The affect of the mechanical environment in some peripheral arteries on stents has been documented. This study quantifies the variation in stresses caused by the mechanical factors described by Diaz *et al*. (Diaz *et al.*, 2004) and shows that this alone could account for the complications experienced in the placement of peripheral stents. The slotted tube design of the stent modelled in this paper gives it a flexibility lower than open cell designs and, despite its previous use in peripheral arteries, is not best suited for placement in an environment where bending will occur. It would be expected that more flexible stent designs would reduce arterial stresses due to bending, but may not resolve the problem of permanent deformation. It is proposed that finite element models such as that presented here could prove to be useful tools for comparing peripheral stent designs in terms of flexibility and stress induced in the vessel wall, as well as for testing new and modified designs in order to reduce stress and damage in the artery. The model also supports the idea that stents should be designed specifically for use in arteries that are subject to significant amounts of bending.

Acknowledgements

This project was funded by an Enterprise Ireland Innovation Partnership grant (IP/2005/0250) and ClearStream Technologies Group.

List of Figures

Figure 1

(a) Geometry of unexpanded stent in stenosed artery, showing stent, plaque and artery. Note that due to symmetry, only a quarter model is used. Stent and artery are constrained in the longitudinal direction half way along the length of the segment (the right-hand side of figure) , and in circumferential direction in the plane that cuts the segment into two semi-cylinders (b) Schematic of spring concept used to model constraint of balloon. (c) Single stent cell, showing location of spring elements.

Figure 2

Stent, plaque and artery geometry showing (a) initial geometry, (b) expanded stent, (c) expanded stent following recoil, (d) application of displacement boundary condition to model 3-point bending of artery. In this case, a single node at the top corner of the artery at the mid-plane (right-hand side of figure) is additionally restrained in all directions, while the end of the artery is displaced downwards. (e) removal of displacement boundary condition.

Figure 3

The dog-boning effect caused by the mechanics of the stent expansion.

Figure 4

Stress volume distribution for stent expanded in an artery with plaque showing results for expansion, recoil and bending.

Figure 5

Stress volume distribution for stent expanded in an artery with no plaque showing results for expansion, recoil and bending.

Figure 6 (a), (b) & (c)

Von Mises stresses in artery (plaque and stent not shown) (a) following stent expansion, and (b) following bending of the artery. (c) Stresses in an unstented artery following bending. Note: stress scales are different.

Figure 7.

The deformed stent following (a) expansion and (b) one bending cycle in the XZ plane and XY plane.

References

Babalik E, Gulbaran M, Gurmen T, Ozturk S. 2003. Fracture of popliteal artery stents. Circ J.67(7):643-5.

Ballyk PD. 2006. Intramural stress increases exponentially with stent diameter: a stress threshold for neointimal hyperplasia. J Vasc Interv Radiol.17(7):1139-45.

Bedoya J, Meyer CA, Timmins LH, Moreno MR, Moore JE. 2006. Effects of stent design parameters on normal artery wall mechanics. J Biomech Eng.128(5):757-65.

Chua SND, Mac Donald BJ, Hashmi MSJ. 2002. Finite-element simulation of stent expansion. Journal of Materials Processing Technology.120(1-3):335-340.

Chua SND, Mac Donald BJ, Hashmi MSJ. 2003. Finite element simulation of stent and balloon interaction. Journal of Materials Processing Technology.143:591-597.

Chua SND, MacDonald BJ, Hashmi MSJ. 2004. Finite element simulation of slotted tube (stent) with the presence of plaque and artery by balloon expansion. Journal of Materials Processing Technology.155-56:1772-1779.

De Beule P, Mortier, P., Segers, S.G., Carlier, B., Verhegghe, R., Van Impe, R., Verdonck, P. 2006. Finite element simulation of the free expansion of the Cypher stent crimped on a tri-folded balloon. Journal of Biomechanics.39(Supplement 1):S297.

Diaz JA, Villegas M, Tamashiro G*, et al.* 2004. Flexions of the popliteal artery: dynamic angiography. J Invasive Cardiol.16(12):712-5.

Ding Z, Friedman MH. 2000. Dynamics of human coronary arterial motion and its potential role in coronary atherogenesis. J Biomech Eng.122(5):488-92.

Ding Z, Friedman MH. 2000. Quantification of 3-D coronary arterial motion using clinical biplane cineangiograms. Int J Card Imaging.16(5):331-46.

Ding Z, Zhu H, Friedman MH. 2002. Coronary artery dynamics in vivo. Ann Biomed Eng.30(4):419-29.

Duda SH, Pusich B, Richter G*, et al.* 2002. Sirolimus-eluting stents for the treatment of obstructive superficial femoral artery disease: six-month results. Circulation.106(12):1505-9.

Duerig TW, Wholey M. 2002. A comparison of balloon- and self-expanding stents. Minimally Invasive Therapy & Allied Technologies.11(4):173-178.

Gay M, Zhang L, Liu WK. 2006. Stent modeling using immersed finite element method. Computer Methods in Applied Mechanics and Engineering.195(33-36):4358-4370.

Hoffmann U, Vetter J, Rainoni L, Leu AJ, Bollinger A. 1997. Popliteal artery compression and force of active plantar flexion in young healthy volunteers. J Vasc Surg.26(2):281-7.

Holzapfel GA, Gasser TC, Ogden RW. 2000. A new constitutive framework for arterial wall mechanics and a comparative study of material models. Journal of Elasticity.61(1-3):1-48.

Holzapfel GA, Stadler M, Gasser TC. 2005. Changes in the mechanical environment of stenotic arteries during interaction with stents: computational assessment of parametric stent designs. J Biomech Eng.127(1):166-80.

Jorgensen E, Kelbaek H, Helqvist S*, et al.* 2003. Low restenosis rate of the NIR coronary stent: results of the Danish multicenter stent study (DANSTENT)--a randomized trial comparing a first-generation stent with a second-generation stent. Am Heart J.145(2):e5.

Kroger K, Santosa F, Goyen M. 2004. Biomechanical incompatibility of popliteal stent placement. J Endovasc Ther.11(6):686-94.

Krueger KD, Mitra AK, DelCore MG, Hunter WJ, 3rd, Agrawal DK. 2006. A comparison of stent-induced stenosis in coronary and peripheral arteries. J Clin Pathol.59(6):575-9.

Lally C, Dolan F, Prendergast PJ. 2005. Cardiovascular stent design and vessel stresses: a finite element analysis. J Biomech.38(8):1574-81.

Laroche D, Delorme S, Anderson T, DiRaddo R. 2006. Computer prediction of friction in balloon angioplasty and stent implantation. Biomedical Simulation, Proceedings.4072:1-8.

Learoyd BM, Taylor MG. 1966. Alterations with age in the viscoelastic properties of human arterial walls. Circ Res.18(3):278-92.

Liang DK, Yang DZ, Qi M, Wang WQ. 2005. Finite element analysis of the implantation of a balloon-expandable stent in a stenosed artery. Int J Cardiol.104(3):314-8.

Martini FH. 2004 Fundamentals of Anatomy and Physiology. 6th ed: Benjamin Cummings.

Matsi PJ, Manninen HI, Soder HK, Mustonen P, Kouri J. 1995. Percutaneous transluminal angioplasty in femoral artery occlusions: primary and long-term results in 107 claudicant patients using femoral and popliteal catheterization techniques. Clin Radiol.50(4):237-44.

Menichelli M, Parma A, Pucci E*, et al.* 2007. Randomized trial of Sirolimus-Eluting Stent Versus Bare-Metal Stent in Acute Myocardial Infarction (SESAMI). J Am Coll Cardiol.49(19):1924-30.

Migliavacca F, Petrini L, Montanari V, Quagliana I, Auricchio F, Dubini G. 2005. A predictive study of the mechanical behaviour of coronary stents by computer modelling. Med Eng Phys.27(1):13-8.

Mills CJ, Gabe IT, Gault JH*, et al.* 1970. Pressure-flow relationships and vascular impedance in man. Cardiovasc Res.4(4):405-17.

Moer R, Myreng Y, Molstad P*, et al.* 2001. Stenting in small coronary arteries (SISCA) trial - A randomized comparison between balloon angioplasty and the heparin-coated beStent. Journal of the American College of Cardiology.38(6):1598-1603.

Mukherjee D, Yadav JS. 2001. Update on peripheral vascular diseases: from smoking cessation to stenting. Cleve Clin J Med.68(8):723-33.

Ormiston JA, Dixon SR, Webster MW*, et al.* 2000. Stent longitudinal flexibility: a comparison of 13 stent designs before and after balloon expansion. Catheter Cardiovasc Interv.50(1):120-4.

Prendergast PJ, Lally C, Daly S*, et al.* 2003. Analysis of prolapse in cardiovascular stents: a constitutive equation for vascular tissue and finite-element modelling. J Biomech Eng.125(5):692-9.

Radegran G, Saltin B. 2000. Human femoral artery diameter in relation to knee extensor muscle mass, peak blood flow, and oxygen uptake. Am J Physiol Heart Circ Physiol.278(1):H162-7.

Rosenfield K, Schainfeld R, Pieczek A, Haley L, Isner JM. 1997. Restenosis of endovascular stents from stent compression. J Am Coll Cardiol.29(2):328-38.

Scheinert D, Scheinert S, Sax J*, et al.* 2005. Prevalence and clinical impact of stent fractures after femoropopliteal stenting. J Am Coll Cardiol.45(2):312-5.

Schillinger M, Sabeti S, Loewe C*, et al.* 2006. Balloon angioplasty versus implantation of nitinol stents in the superficial femoral artery. N Engl J Med.354(18):1879-88.

Schwartz R, Holmes, D.R. 1994. Pigs, dogs, baboons and man; Lessons in stenting from animal studies. Journal of Interventional Cardiology.7:355-368.

Solis J, Allaqaband S, Bajwa T. 2006. A case of popliteal stent fracture with pseudoaneurysm formation. Catheter Cardiovasc Interv.67(2):319-22.

Squire JC. Dynamics of endovascular stent expansion. Massachusetts: Massachusetts Institute of Technology; 2000.

Strecker EP, Boos IB, Gottmann D. 1997. Femoropopliteal artery stent placement: evaluation of long-term success. Radiology.205(2):375-83.

Takashima K, Kitou T, Mori K, Ikeuchi K. 2007. Simulation and experimental observation of contact conditions between stents and artery models. Med Eng Phys.29(3):326-35.

Wang WQ, Liang DK, Yang DZ, Qi M. 2006. Analysis of the transient expansion behavior and design optimization of coronary stents by finite element method. J Biomech.39(1):21-32.

Weydahl ES, Moore JE. 2001. Dynamic curvature strongly affects wall shear rates in a coronary artery bifurcation model. J Biomech.34(9):1189-96.

Wiersma S, Dolan F, Taylor D. 2006. Fatigue and fracture in materials used for micro-scale biomedical components. Biomed Mater Eng.16(2):137-46.

Zeng D, Ding Z, Friedman MH, Ethier CR. 2003. Effects of cardiac motion on right coronary artery hemodynamics. Ann Biomed Eng.31(4):420-9.

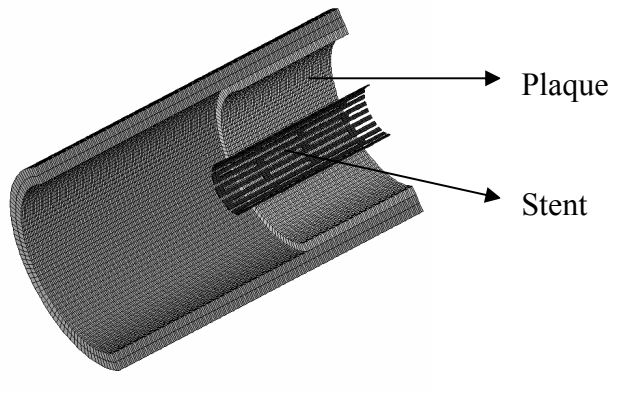

Figure 1
Geometry of unexpanded stent in stenosed artery, showing stent, plaque and artery. Note that due to symmetry, only a quarter model is used.

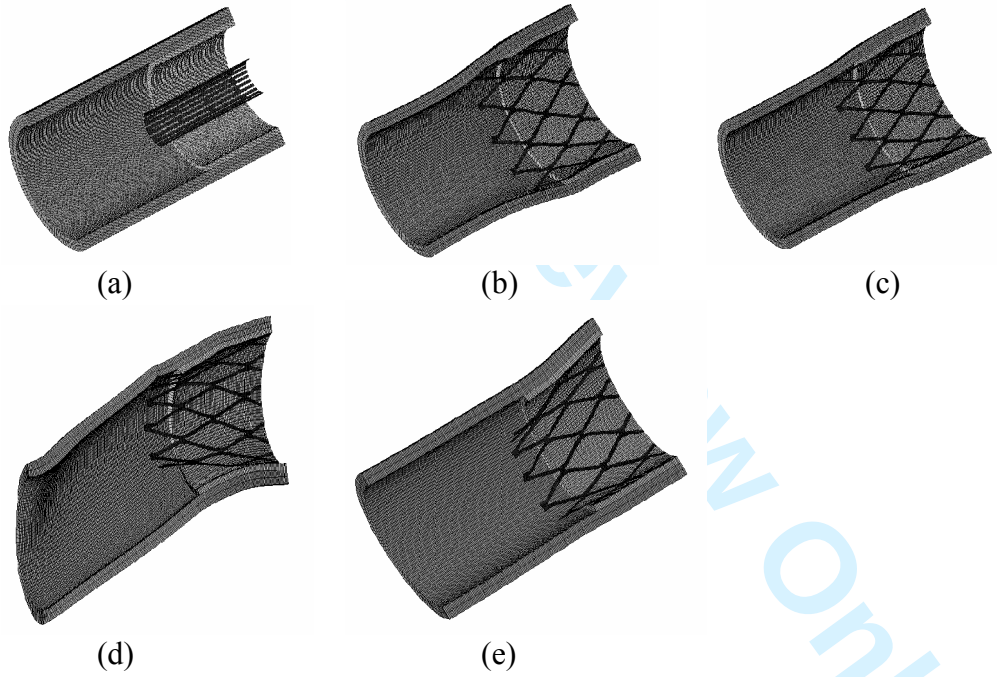

Figure 2
Stent, plaque and artery geometry showing (a) initial geometry, (b) expanded stent, (c) expanded stent following recoil, (d) application of bending boundary condition and (e) removal of bending boundary condition

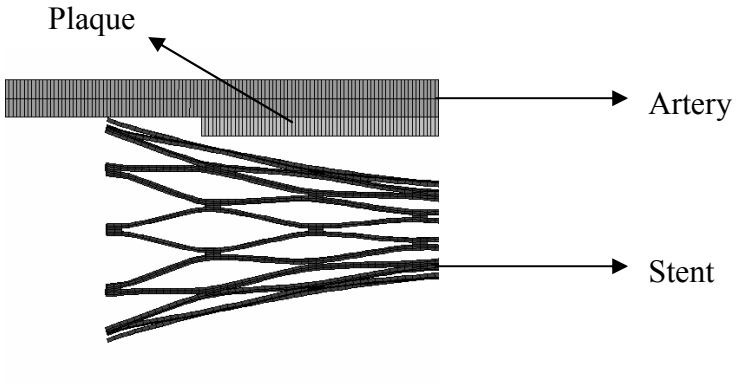

Figure 3
The dog-boning effect caused by the mechanics of the stent expansion.

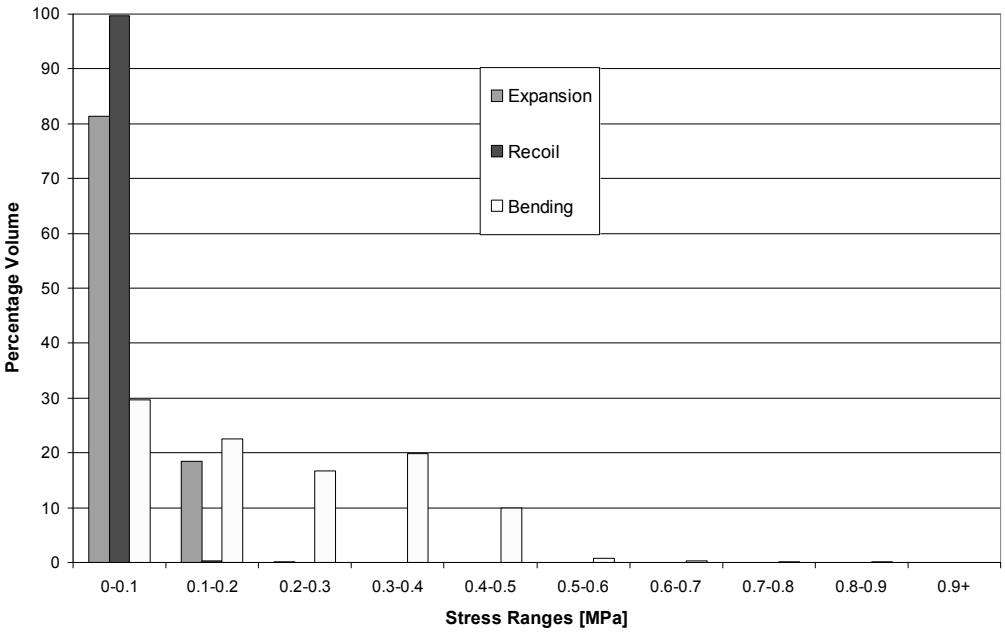

Figure 4
Stress volume distribution for stent expanded in an artery with plaque showing results for expansion, recoil and bending.

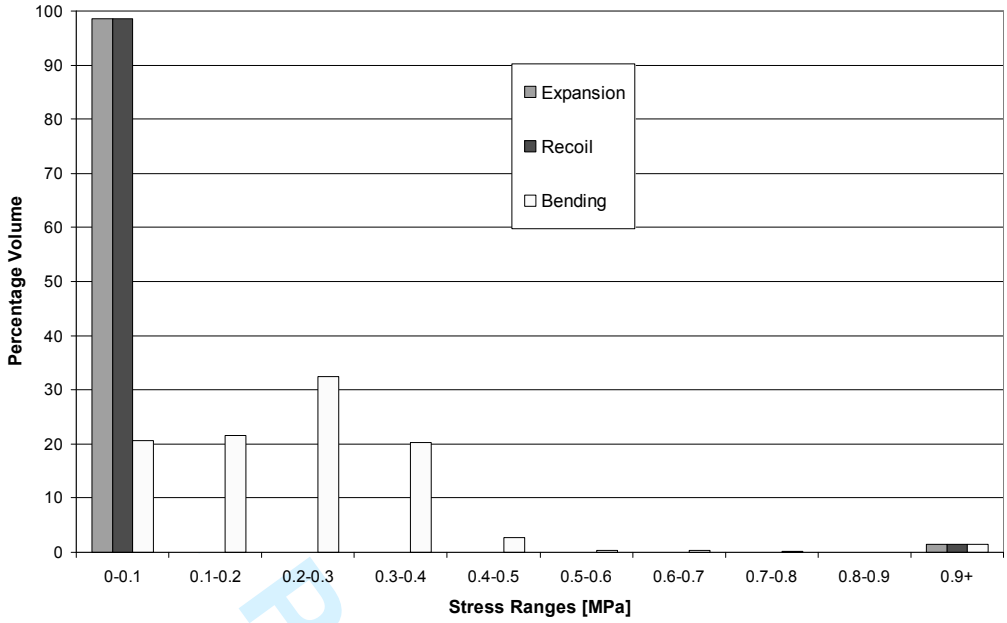

Figure 5
Stress volume distribution for stent expanded in an artery with no plaque showing results for expansion, recoil and bending.

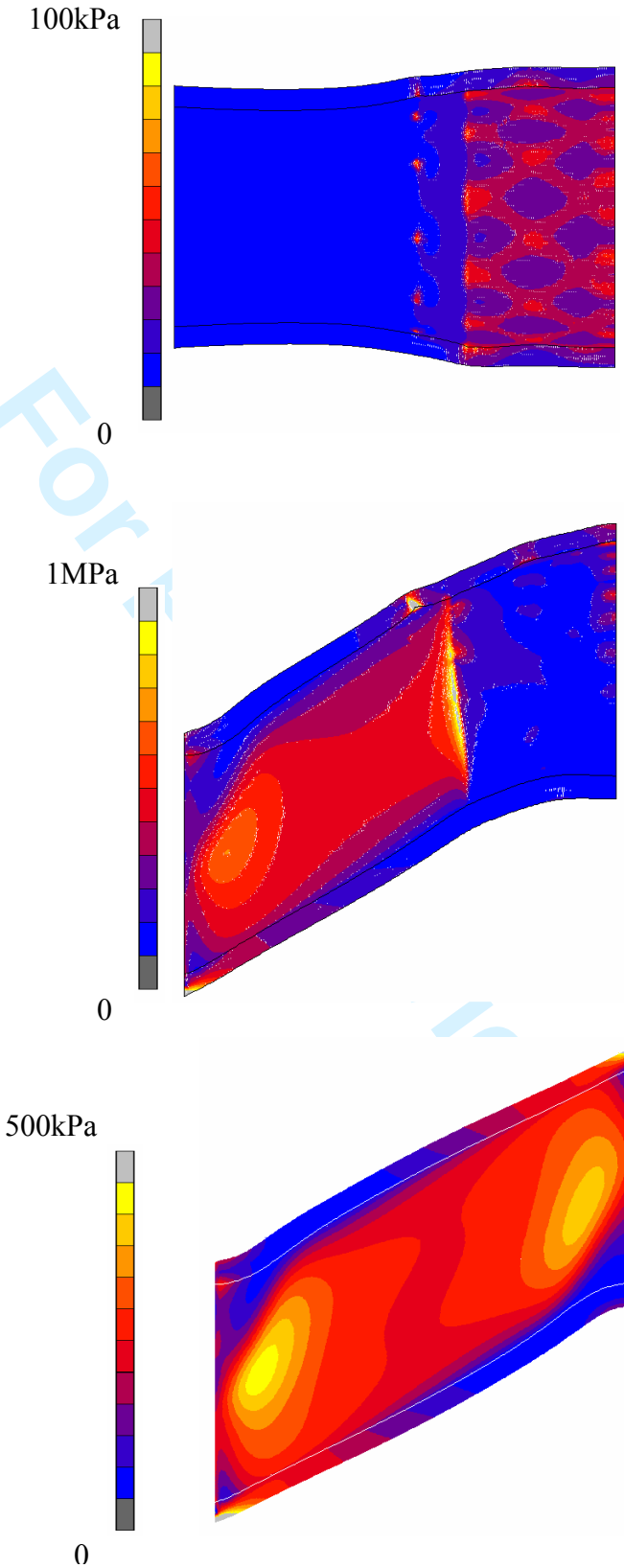

Figure 6 (a), (b) & (c)
Von Mises stresses in artery (plaque and stent not shown) (a) following stent expansion, and (b) following bending of the artery. (c) Stresses in an unstented artery following bending. Note: stress scales are different.

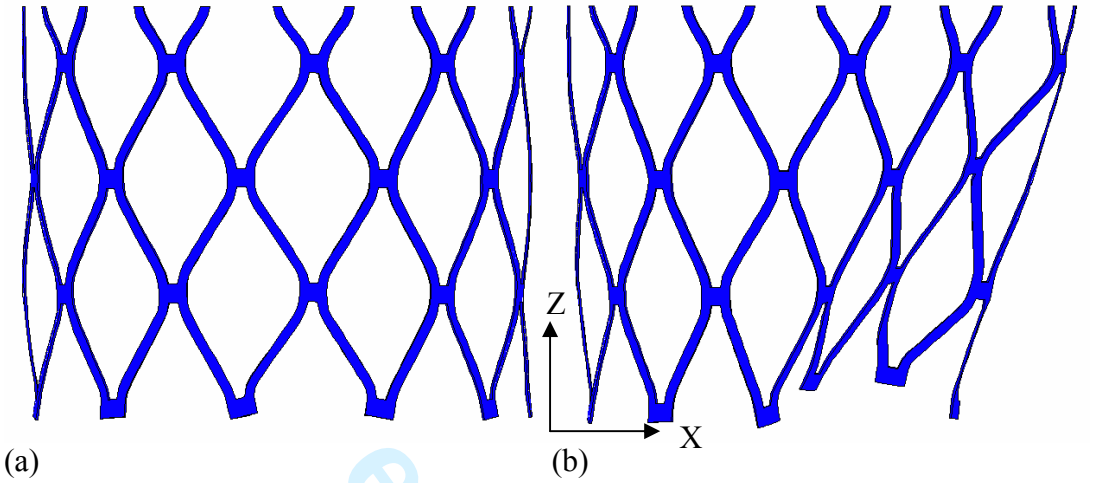

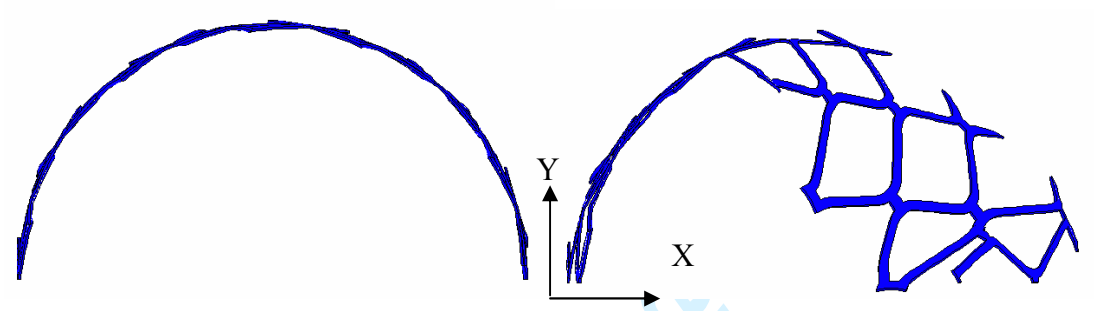

Figure 7 (a) & (b)
The deformed stent following (a) expansion and (b) one bending cycle from two different views